Eur Radiol (2004) 14:1241–1248
DOI 10.1007/s00330-003-2203-2

Emmanuel Coche
Franck Verschuren
Philippe Hainaut
Louis Goncette

Pulmonary embolism findings on chest radiographs and multislice spiral CT

Received: 25 June 2003
Revised: 7 November 2003
Accepted: 1 December 2003
Published online: 17 February 2004

E. Coche (✉) · L. Goncette
Department of Radiology,
Cliniques Universitaires Saint-Luc,
Université Catholique de Louvain,
Avenue Hippocrate 10, 1200 Brussels,
Belgium
e-mail: coche@rdgn.ucl.ac.be
Tel.: +32-2-7642926
Fax: +32-2-7705574

F. Verschuren
Department of Intensive Care
and Emergency Medicine,
Cliniques Universitaires Saint-Luc,
Université Catholique de Louvain,
Avenue Hippocrate 10, 1200 Brussels,
Belgium

P. Hainaut
Department of Internal Medicine,
Cliniques Universitaires Saint-Luc,
Université Catholique de Louvain,
Avenue Hippocrate 10, 1200 Brussels,
Belgium

Abstract Multislice spiral CT is becoming an increasingly important tool for diagnosing pulmonary embolism. However, in many instances, a chest radiograph is usually performed as a first-line examination. Many parenchymal, vascular, and other ancillary findings may be observed on both imaging modalities with a highly detailed depiction of abnormalities on multislice CT. A comprehensive review of chest radiograph findings is presented with side-by-side correlations of CT images reformatted mainly in the frontal plane.

Keywords Multislice CT · Pulmonary embolism · Chest radiograph

Introduction

A chest radiograph is usually the first imaging study performed in patients with suspected pulmonary embolism (PE). Chest radiographs have limited value in establishing or excluding the diagnosis of PE [1]. However, this imaging modality is helpful in excluding diagnoses of diseases that may clinically mimic PE. Some authors have reported several findings that were attributed to the presence of PE [2–8] on plain chest radiographs and later on computed tomography (CT) images [9–14]. Some correlations with autopsy and radiographic findings [7] were made to understand better the parenchymal and vascular abnormalities seen on chest radiographs.

Over the past 10 years, spiral CT angiography has reached a high accuracy in the evaluation of PE [15, 16] and in the potential assessment of its severity [17, 18]. The use of multislice CT for the detection of PE allows acquisition of the entire chest in one breath-hold using thin slices, resulting in increased image quality [19]. At present, radiologists have the opportunity to correlate the different abnormalities seen on chest radiographs with images obtained with mutlislice CT. In this pictorial es-

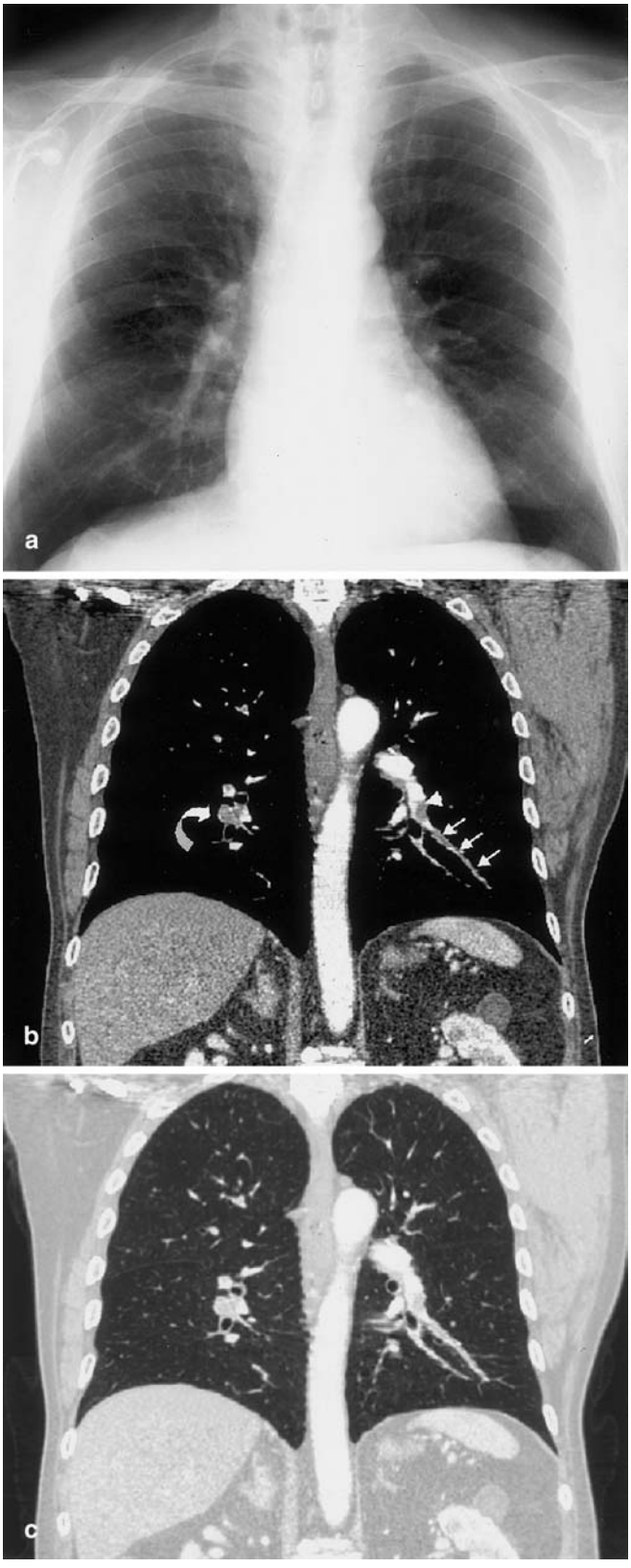

Fig. 1a–c Acute PE in an 80-year-old man. **a** Frontal chest X-ray is normal **b** Coronal reconstruction image obtained with multislice CT (soft-tissue window settings, 1.3 mm collimation, 0.6 mm interval reconstruction) reveals multiple emboli located in the left inferior artery (*arrowhead*) and laterobasal artery (*straight arrows*). Note occlusion of the right inferior pulmonary artery by a large clot (*curved arrow*). **c** Coronal reconstruction image obtained with multislice CT (lung-tissue window settings, 1.3 mm collimation, 0.6 mm interval reconstruction) did not show any parenchymal abnormality

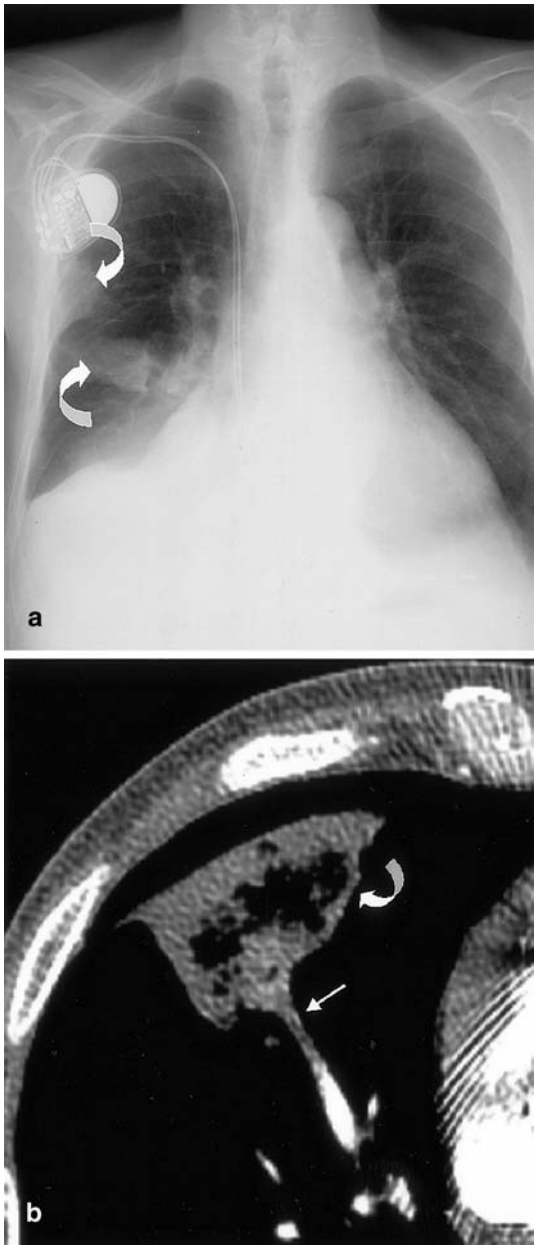

Fig. 2a, b A 72-year-old man with recurrent chest pain and dyspnea. This patient had previous thromboembolic disease treated with anticoagulation and inferior cava filter placement. **a** Frontal chest X-ray reveals cardiac enlargement with pacemaker. Well-defined densities are present in the axillar portion of the right lung (*curved arrows*) in a configuration compatible with pulmonary infarcts. **b** Axial view of thin-section multislice CT (soft-tissue window settings, 1.3 mm collimation, 0.6 mm interval reconstruction) revealed the inferior pleural-based (minor fissure) wedge-shaped opacity partially aerated in the right middle lobe (*curved arrow*). The peripheral artery leading to it was thrombosed (*straight arrow*). The diagnosis of recurrent PE with pulmonary infarct was established

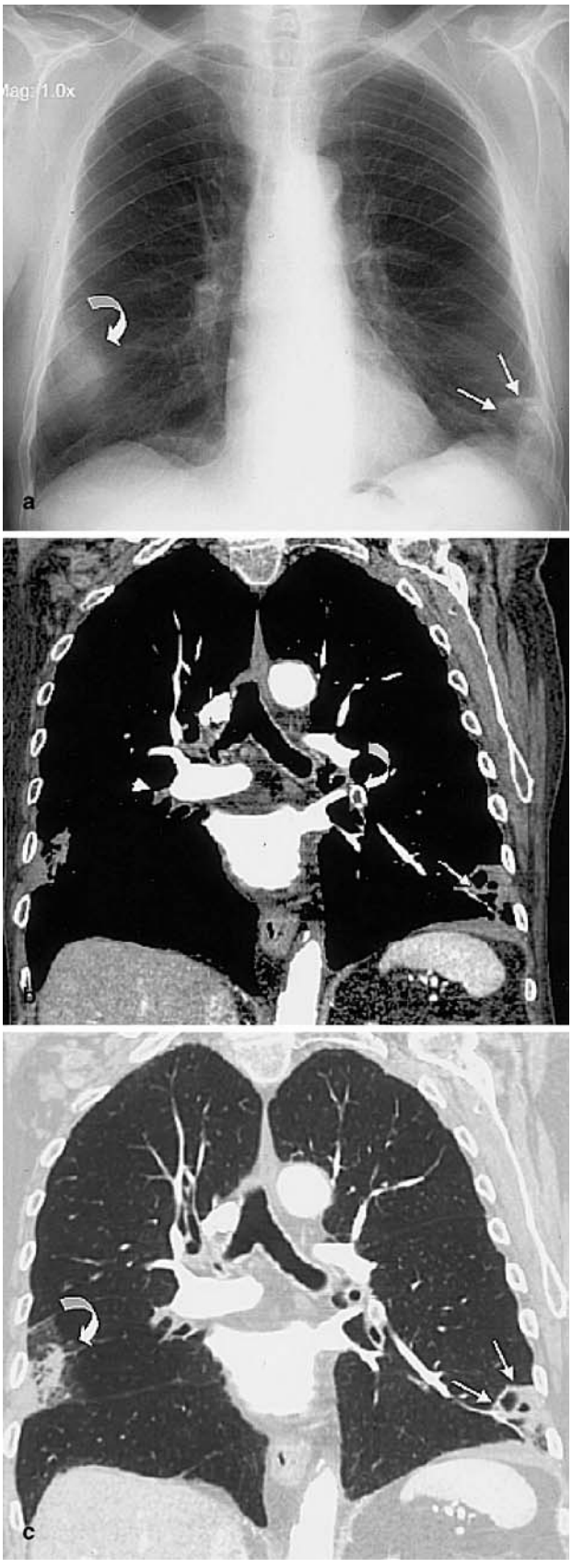

say we present a comprehensive analysis of abnormalities seen mainly on coronal reformatted images obtained with multislice CT.

Chest radiographs and multislice CT

Chest radiographs were obtained by using a 150-cm source–image distance (Thoramat, Siemens, Erlangen, Germany). Most of the patients had an erect postero-anterior chest radiograph. All CT images were obtained within 24 h on commercially available multislice CT equipment (MX 8000, Philips Medical Systems, Cleveland, Ohio). The scanning parameters were as follows: 0.5 s scan time, 4×1 mm section thickness, pitch of 1.25, 120 Kv, and 144 mA s. All studies were performed with 100–140 cc nonionic intravenous contrast medium administered at 3 ml/s and a variable start-delay. All patients underwent craniocaudal scanning; the *z*-axis coverage and the field of view were chosen to include the entire thorax from the apex to the bases of the lung parenchyma. Multiplanar reconstructions were performed in frontal projections to provide the same view as that represented by postero-anterior chest X-rays. The plane of reconstruction was selected to represent better the abnormalities seen on the chest radiograph. PE was considered present on multislice CT when a filling defect was seen in the pulmonary artery or in its branches of division.

Acute pulmonary embolism

Normal chest radiograph

A chest X-ray is normal in a small number of patients with acute PE (Fig. 1). Worsley et al. [6] reviewed the chest radiograph findings of 1,063 patients with suspected

Fig. 3a–c An 82-year-old man with right iliac vein thrombosis. **a** Frontal chest X-ray shows ill-defined densities in the lower portion of the right and left lungs (*curved and straight arrows*). **b** Coronal reconstruction image obtained with multislice CT (soft-tissue window settings, 1.3 mm collimation, 0.6 mm interval reconstruction) revealed pleural-based wedge-shaped opacity in the external segment of the right middle lobe and laterobasal segment of the left lower lobe. The peripheral artery leading to the laterobasal segment of the left lower lobe was thrombosed (*straight arrow*). Note the embolus located at the initial portion of the left lower artery (*curved arrow*) and at the origin of the lateral artery of the right middle lobe (*arrowhead*). **c** Coronal reconstruction image obtained with multislice CT (lung-tissue window settings, 1.3 mm collimation, 0.6 mm interval reconstruction) revealed a partially excavated opacity in the left lower lobe (*arrows*), consistent in this context with semi-acute PE. The right opacity (*curved arrow*) was surrounded by ground-glass opacities consistent with alveolar hemorrhage as frequently encountered in acute PE

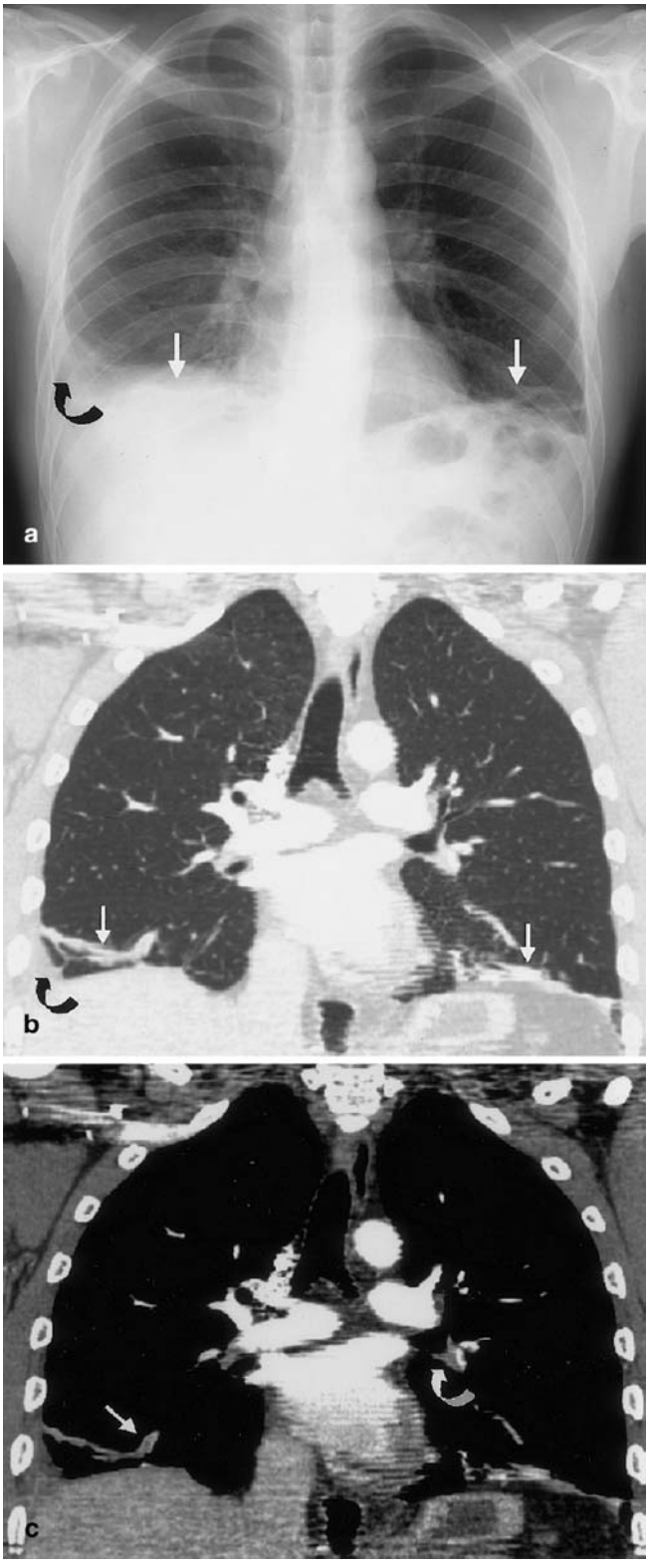

Fig. 4a–c A 36-year-old man with vague thoracic pain and mild dyspnea. Treatment with antibiotics was unsuccessful. **a** Frontal chest X-ray reveals linear densities in both lower lobes. The radiological appearance was consistent with atelectasis (*straight arrows*). Pleural effusion was noted on the right side (*curved arrow*). **b** Coronal reconstruction image obtained at the level of the carina with multislice CT (lung-tissue window settings, 1.3 mm collimation, 0.6 mm interval reconstruction) reveals bilateral peripheral atelectasis (*straight arrows*) with a minimal right pleural effusion (*curved arrow*). **c** Coronal reconstruction image obtained at the level of the carina with multislice CT (soft-tissue window settings, 1.3 mm collimation, 0.6 mm interval reconstruction) depicts the embolus (*straight arrow*) occupying the peripheral segment of the right anterobasal artery. A clot is identified in the left inferior pulmonary artery (*curved arrow*)

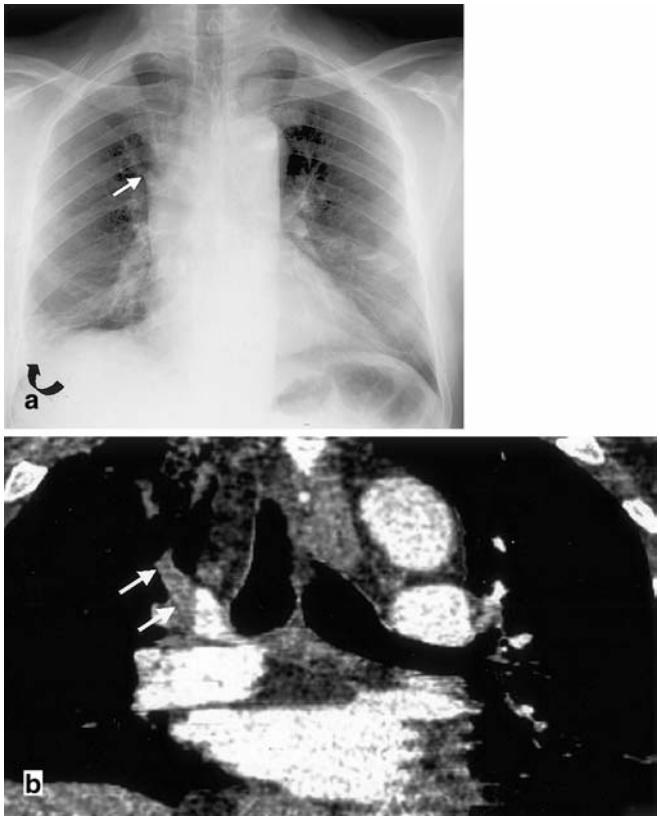

Fig. 5a, b A 45-year-old man with right thoracic pain, dyspnea, and hemoptysis. **a** Frontal chest X-ray does not reveal any parenchymal abnormalities. Right pleural effusion is present (*curved arrow*). The right upper lobe artery appears enlarged in its initial portion (Fleischner's sign) and then amputated (knuckle sign; *straight arrow*). **b** Magnified view of the coronal reconstruction image obtained at the level of the right upper lobe artery with multislice CT (soft-tissue window settings, 1.3 mm collimation, 0.6 mm interval reconstruction) reveals complete vascular occlusion of the right upper lobe artery (*straight arrows*), just after its origin

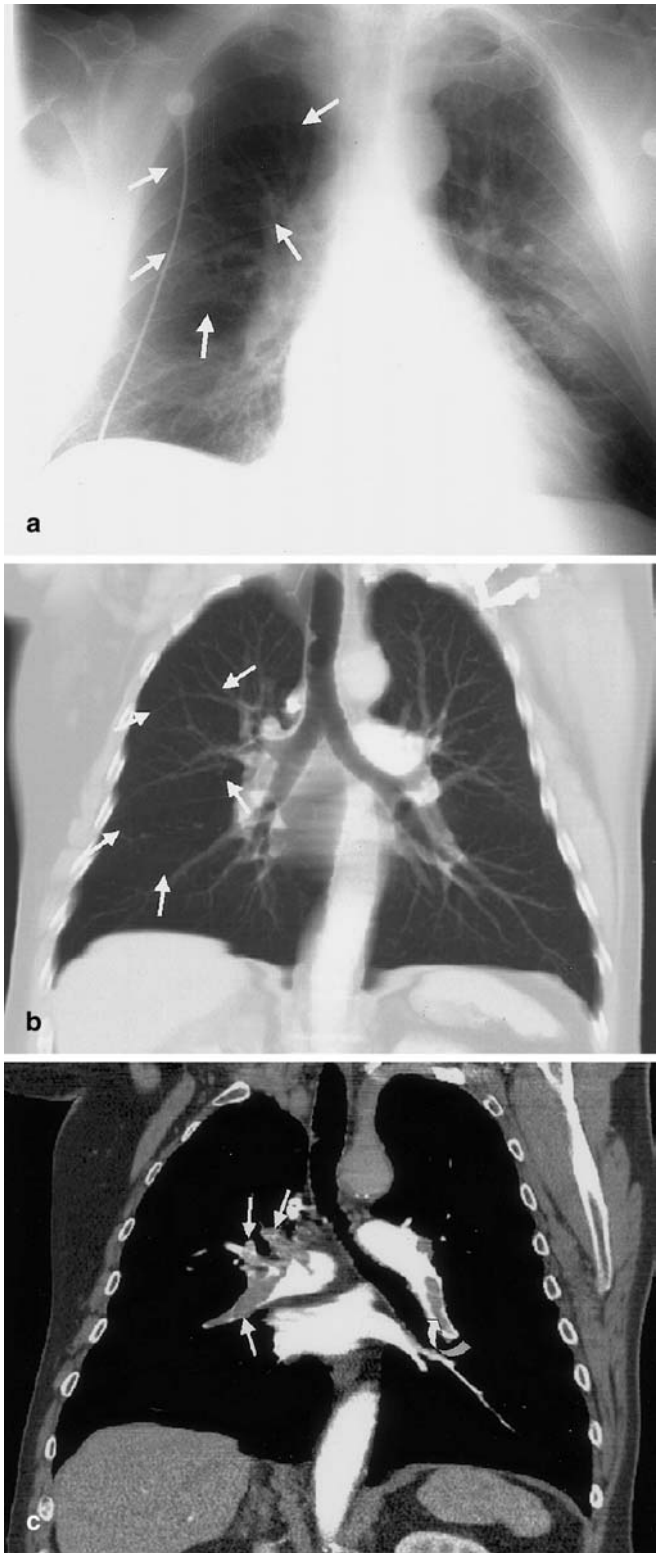

Fig. 6a–c A 69-year-old man admitted in emergency for mild dyspnea, without evidence of deep venous thrombosis. D-Dimers were above 1,000 ng/ml. **a** Bedside chest X-ray reveals right upper lobe hyperlucency (*straight arrows*; Westermark's sign) without any other parenchymal or pleural abnormalities. **b** Coronal reconstruction image obtained at the level of the carina with multislice CT (lung-tissue window settings, 1.3 mm collimation, 10 mm slice thickness reconstruction) confirms the hyperlucency of the right lung (*straight arrows*) compared to the opposite side. **c** Coronal reconstruction image obtained at the level of the right and left main pulmonary arteries with multislice CT (soft-tissue window settings, 1.3 mm collimation, 0.6 mm interval reconstruction) demonstrates the emboli (*straight arrows*) occluding the right pulmonary artery and its branches. A large clot was also present in the left inferior pulmonary artery (*curved arrow*)

PE during the PIOPED study and found a normal chest radiograph in 12% of patients with PE confirmed by pulmonary angiography. The international cooperative PE registry [8] reported 24% normal chest radiographs in 2,452 consecutive patients who had received a diagnosis of acute PE.

Pulmonary infarction

A pulmonary infarct usually resembles a truncated cone (Hampton's hump). It consists of homogeneous wedge-shaped consolidation located in the lung periphery [7–12] (Fig. 2). It may be surrounded by ground-glass opacity (Fig. 3). The range of pulmonary infarcts seen on chest radiographs for patients admitted with acute PE is between 5 and 10%. Their relative frequency is influenced by the time interval between the onset of symptoms, the performance of chest radiography, and the severity of PE [8]. Cavitation may occur several weeks after the acute event (Fig. 3) [7].

Parenchymal consolidation and volume loss

The most common chest radiographic finding in patients with PE is atelectasis and/or parenchymal areas of increased opacity [6–8] (Fig. 4). The consolidation may result from edema or hemorrhage with or without pulmonary infarction [7, 11]. Nonwedge-shaped consolidation and atelectasis occur in 19 and 35% of patients with PE, respectively [10]. Elevation of the hemidiaphragm in relationship with loss of lung volume may be observed in 50% of patients within 24 h of onset of symptoms and in 15% of patients with symptoms of longer duration [7].

Enlargement of pulmonary arteries and amputation of occluded vessels

A clot occupying a vessel enlarges its diameter at least in its acute stage. Enlargement of central pulmonary arteries is called Fleischner's sign [7]. This enlargement is

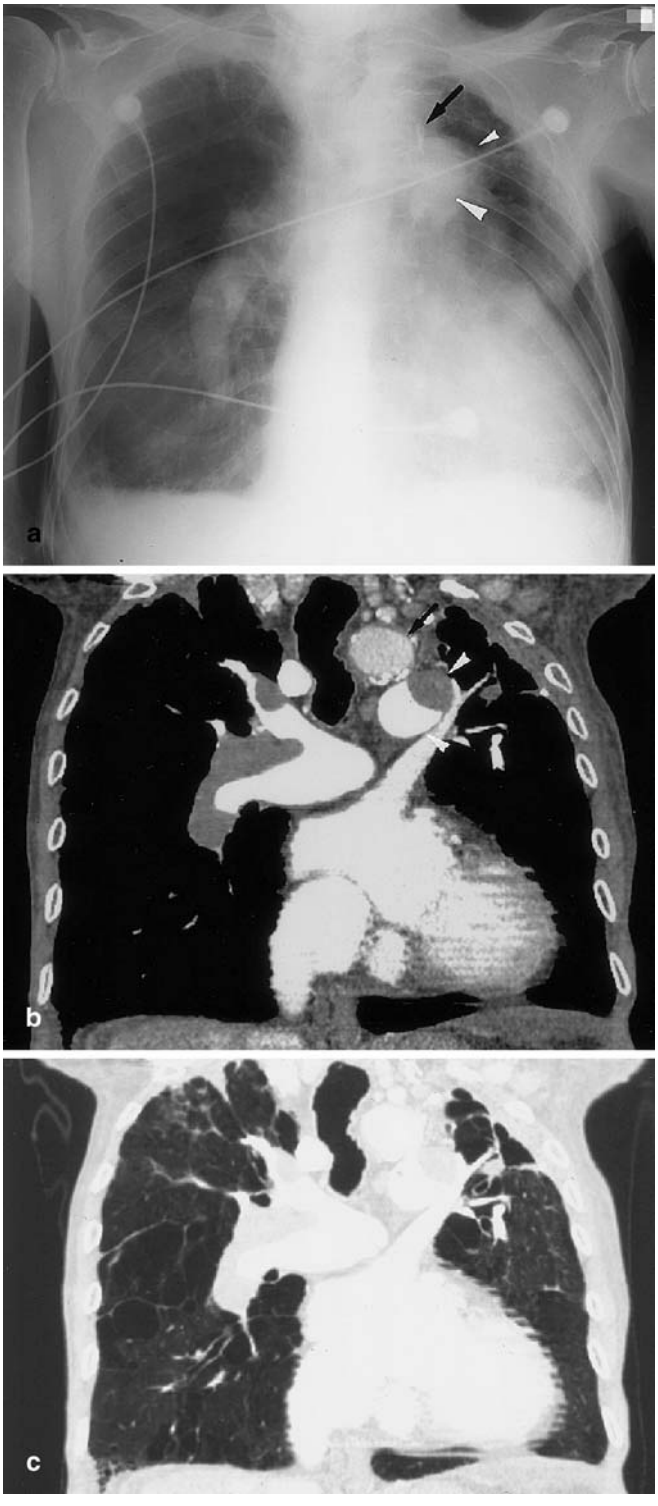

Fig. 7a–c A 75-year-old man with pulmonary hypertension. **a** Frontal chest X-ray reveals cardiomegaly with overinflated and hyperlucent lung on the right side. The right pulmonary artery is obviously enlarged. The left pulmonary artery is dilated (*arrowheads*) and partially masked by the calcified aortic arch (*black straight arrow*). Note the extensive thickening of the pleura in the left apical and axillary regions and right upper lobe scarring. **b** Coronal reconstruction image obtained at the level of the proximal pulmonary arteries with multislice CT (soft-tissue window settings, 1.3 mm collimation, 0.6 mm interval reconstruction) revealed large excentric thrombi in proximal pulmonary arteries consistent with chronic PE. Note the dilated left pulmonary artery (*arrowheads*) adjacent to the aortic arch (*black straight arrow*) as observed on the standard chest X-ray. **c** Coronal reconstruction image obtained at the level of the right pulmonary artery with multislice CT (lung-tissue window settings, 1.3 mm collimation, 0.6 mm interval reconstruction) reveals severe emphysema contributing to the hyperlucency of the right lung

caused directly by the clot itself rather than by the induced pulmonary hypertension. The abrupt tapering of the occluded vessel distally is known as the so-called knuckle sign [3] (Fig. 5).

Focal oligemia

Massive pulmonary emboli may obstruct blood flow through the main pulmonary artery, producing bilaterally hyperlucent lungs, but fortunately, this is a rare occurrence. More localized areas of hyperlucency (Fig. 6) called Westermark's sign [2] may result from smaller pulmonary emboli. These areas of hyperlucency may be segmental, lobar, or involve an entire lung.

Pleural effusion

Pleural effusion is seen in 35–55% of patients who have acute PE (Figs. 4, 5). It was shown that the side of pleural effusion is not correlated with the side of PE [10].

Chronic pulmonary embolism

Chronic PE is a rare but serious complication of acute PE. Angiospiral CT is helpful for diagnosis, particularly in proximal locations (Fig. 7) accessible to surgical treatment by thomboendarterectomy. The classic radiographic findings associated with pulmonary artery hypertension and concomitant chronic PE include pulmonary artery enlargement, right heart enlargement, areas of decreased pulmonary vascularity, enlargement of the azygos vein, pleural effusion and/or atelectasis, and pleural thickening [13, 20, 21] (Fig. 7). Calcifications have been reported to occur in long-standing pulmonary arterial clots (Fig. 8). Mosaic perfusion related to redistribution of vascularization [14] has been described on CT images but is not visible on standard chest radiographs.

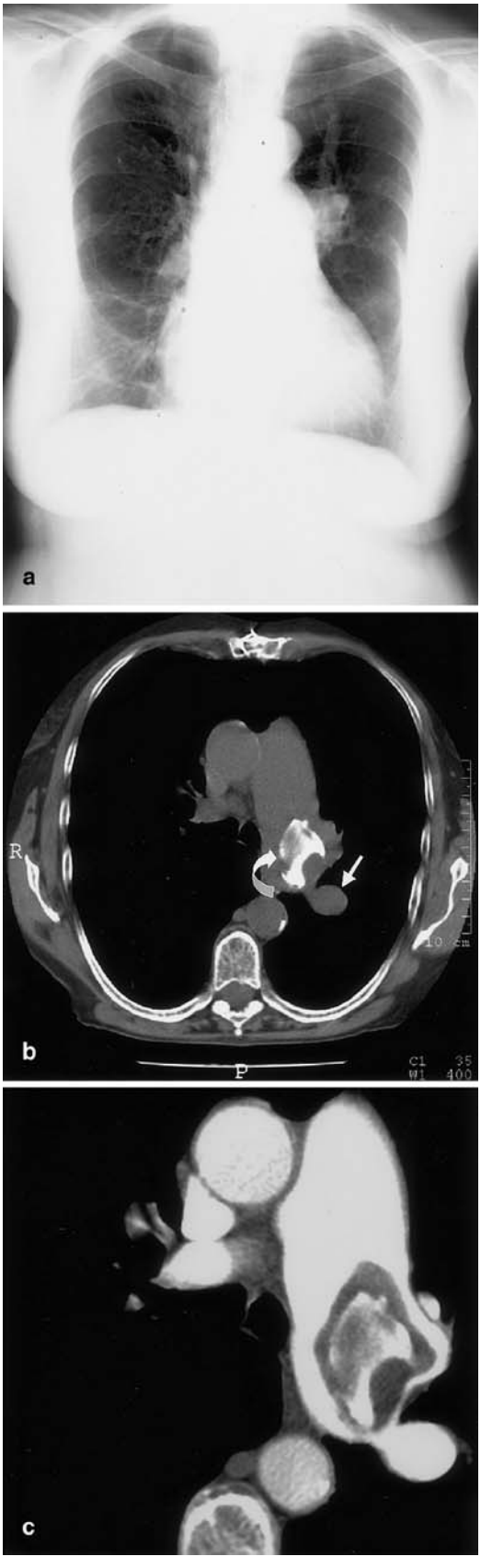

Conclusion

Acute and chronic PE may cause many different signs on chest radiographs. Most of these signs are nonspecific and others are subtle and difficult to recognize. Thin-collimation multislice CT is a powerful imaging technique for the detection of PE and for the depiction of associated chest abnormalities. Side-by-side comparison of chest radiographs and reformatted images obtained with multislice CT helps the radiologist to understand and recognize these findings on chest radiographs.

Fig. 8a–c A 71-year-old woman with progressive dyspnea. **a** Frontal chest X-ray reveals marked enlargement of the central pulmonary arteries. **b** Unenhanced axial CT obtained at the level of the left main pulmonary artery shows a large intravascular calcified thrombus (*curved arrow*) not seen on the chest X-ray. The left pulmonary artery was dilated measuring 44 mm in diameter. The apicodorsal branch of the culminal artery (*short arrow*) appeared dilated. **c** Magnified view of enhanced axial CT obtained at the same level as **b** shows the noncalcified portion of the large thrombus consistent with long-standing chronic PE

References

1. Greenspan RH, Ravin CE, Polansky SM, McLoud TC (1982) Accuracy of chest radiograph in diagnosis of pulmonary embolism. Invest Radiol 17:539–543
2. Westermark N (1938) On the Roentgen diagnosis of lung embolism. Acta Radiol 19:357
3. Williams JR, Wilcox WC (1963) Pulmonary embolism: roentgenographic and angiographic considerations. AJR 89:333–342
4. Bedard CK, Bone RC (1977) Westermark's sign in the diagnosis of pulmonary emboli in patients with the adult respiratory distress syndrome. Crit Care Med 5:137–140
5. Buckner CB, Walker CW, Purnell GL (1989) Pulmonary embolism: chest radiographic abnormalities. J Thorac Imag 4:23–27
6. Worsley DF, Alavi AA, Aronchick JM et al (1993) Chest radiographic findings in patients with acute pulmonary embolism: observations from the PIOPED study. Radiology 189:133–136
7. Fraser RS, Müller NL, Colman N, Paré PD (1999) Embolic lung disease. In: Fraser RS, Paré PD (eds) Diagnosis diseases of the chest, 4th edn. Saunders, Philadelphia, pp 1773–1843
8. Elliot CG, Goldhaber SZ, Visani L, DeRosa M (2000) Chest radiographs in acute pulmonary embolism. Results from the International Cooperative Pulmonary Embolism Registry. Chest 118:33–38
9. Sinner WN (1978) Computed tomography patterns of pulmonary thromboembolism and infarction. J Comput Assist Tomogr 2:395–399
10. Coche EE, Muller NL, Kim KI, Wiggs BR, Mayo JR (1998) Acute pulmonary embolism: ancillary findings at spiral CT. Radiology 207:753–758
11. Johnson PT, Wechsler RJ, Salazar AM, Fisher AM, Nazarian LN, Steiner RM (1999) Spiral CT of acute pulmonary thromboembolism: evaluation of pleuroparenchymal abnormalities. J Comput Assist Tomogr 23:369–373
12. Shah AA, Davis SD, Gamsu G, Intriere L (1999) Parenchymal and pleural findings in patients with and patients without acute pulmonary embolism detected at spiral CT. Radiology 211:147–153
13. Schmidt HC, Kauczor HU, Schild HH et al (1996) Pulmonary hypertension in patients with chronic pulmonary thromboembolism: chest radiograph and CT evaluation before and after surgery. Eur Radiol 6:817–825
14. Greaves SM, Hart EM, Brown K, Young DA, Batra P, Aberle DR (1995) Pulmonary thromboembolism: spectrum of findings on CT. AJR 165:1359–1363
15. Ghaye B, Remy J, Remy-Jardin M (2002) Non-traumatic thoracic emergencies: CT diagnosis of acute pulmonary embolism: the first 10 years. Eur Radiol 12:1886–1905
16. Ruiz Y, Caballero P, Caniego JL et al (2003) Prospective comparison of helical CT with angiography in pulmonary embolism: global and selective vascular territory analysis. Interobserver agreement. Eur Radiol 13:823–829
17. Mastora I, Remy-Jardin M, Masson P et al (2003) Severity of acute pulmonary embolism: evaluation of a new spiral CT angiographic score in correlation with echocardiographic data. Eur Radiol 13:29–35
18. Collomb D, Paramelle PJ, Calaque O et al (2003) Severity assessment of acute pulmonary embolism: evaluation using helical CT. Eur Radiol 13:1508–1514
19. Remy-Jardin M, Tillie-Leblond I, Szapiro D et al (2002) CT angiography of pulmonary embolism in patients with underlying respiratory disease: impact of multislice CT on image quality and negative predictive value. Eur Radiol 12:1971–1978
20. Woodruff WW 3rd, Hoeck BE, Chitwood WR Jr, Lyerly HK, Sabiston DC Jr, Chen JT (1985) Radiographic findings in pulmonary hypertension from unresolved embolism. AJR 144:681–686
21. Schmidt HC, Kauczor HU, Schild HH, Renner C, Kirchhoff E, Lang P, Iversen S, Thelen M (1996) Pulmonary hypertension in patients with chronic pulmonary thromboembolism: chest radiograph and CT evaluation before and after surgery. Eur Radiol 6:817–825